

## Process conditions for complete decomposition of CHF<sub>3</sub> in a dielectric barrier discharge reactor

Duc Ba Nguyen and Won Gyu Lee<sup>†</sup>

Department of Chemical Engineering, Kangwon National University, Chuncheon, Kangwon 24341, Korea

(Received 4 September 2015 • accepted 6 November 2015)

**Abstract**—Plasma decomposition of CHF<sub>3</sub> was investigated using a dielectric barrier discharge immersed in an electrically insulating oil bath in a mixture of CHF<sub>3</sub>, O<sub>2</sub>, and N<sub>2</sub>. CHF<sub>3</sub> was well decomposed under a relatively high applied voltage in an atmospheric pressure plasma system. The main by-product was CO<sub>2</sub> and its selectivity increased with a decrease in the CHF<sub>3</sub> concentration in the feed. Complete decomposition of CHF<sub>3</sub> was achieved at a typical process range: an applied voltage  $\geq 7.0$  kVp, an initial CHF<sub>3</sub> flow rate of 3 ml/min, and a total flow rate of 500 ml/min. The value of energy efficiency and energy density at the center range for the complete decomposition of CHF<sub>3</sub> was 0.01 mmol/kJ and 6.00 kWh/Nm<sup>3</sup>, respectively.

Keywords: CHF<sub>3</sub>, Dielectric Barrier Discharge, Plasma, Decomposition of CHF<sub>3</sub>, Electrically Insulating Oil

### INTRODUCTION

Even though CHF<sub>3</sub> has wide industrial applications, it has the second highest global warming potential and a long lifetime of 260 years [1]. Several abatement techniques for CHF<sub>3</sub> have been suggested, such as thermal processes [2,3], catalysts [4,5], plasma [6,7], and conversion to environmentally benign compounds [8]. A thermal process is an effective method for the decomposition of CHF<sub>3</sub>, and has been used widely under the clean development mechanism methodologies (CMD) [9,10]. However, due to the formation of several fluorinated compounds in the exhaust gas stream, further processes are needed to treat exhaust before gas waste is emitted into the atmosphere. Among the techniques, a plasma process showed highly potential advantages, because its reactivity yields a higher reaction rate with economic power consumption compared to other methods. Non-thermal plasma and low pressure plasma technology, such as surface wave plasma, arc plasma, and microwave plasma, have been investigated as a technology for fluorocarbons abatement. An atmospheric pressure plasma processing system was designed to evaluate the effectiveness of CHF<sub>3</sub> decomposition, which operates at a lower cost compared to the low pressure plasmas that require more equipment [11-13]. CHF<sub>3</sub> decomposition can be performed under the benign conditions of low process temperature and atmospheric pressure in a dielectric barrier discharge (DBD) [12].

In this study, CHF<sub>3</sub> decomposition was carried out in a coaxial DBD reactor with the reactor immersed in an electrically insulating oil bath. We then investigated the applied voltage, CHF<sub>3</sub> flow rate and total flow rate on the complete CHF<sub>3</sub> decomposition reaction. The influence of several process parameters on the reactivity was also evaluated in the terms of discharge power, reactor tem-

perature, energy density, energy efficiency, CHF<sub>3</sub> decomposition, and selectivity of products (CO, CO<sub>2</sub>, and byproducts).

### EXPERIMENTAL

A schematic reactor diagram for CHF<sub>3</sub> decomposition and the equivalent circuit model of the DBD system are shown in Fig. 1. The coaxial DBD reactor had a fixed discharge gap of 1.0 mm and a discharge volume of 10 ml. The DBD reactor immersed in an electrically insulating oil bath was previously described elsewhere [14]. A mixture of CHF<sub>3</sub>, O<sub>2</sub> and N<sub>2</sub> with a purity of 99.99% was introduced into the discharge zone by mass flow controllers (MKP, TSC-210). Plasma discharge was ignited by an AC pulse power supply (HVP, AP Plasma Power Supply). Applied voltage was measured by a passive high voltage probe (Tektronix, P6015A), while the total current was measured by a Rogowski coil (Pearson, model 410). All electrical data were recorded by an oscilloscope (Tektronix, TDS 2012B) as the waveforms of voltage and current, root mean square of voltage ( $V_{RMS}$ ) and current ( $I_{RMS}$ ), and discharge power (mean of math of voltage x current). Typical voltage, current and discharge power waveforms were generated under an applied voltage of 6.7 kVp, a frequency of 30 kHz; a flow rate of CHF<sub>3</sub> of 5 ml, O<sub>2</sub> of 10 ml and N<sub>2</sub> of 985 ml/min as shown in Fig. 2. The number of micro-discharges per second was exactly sixty thousand times. According to AC Ohm's Law, the absolute impedance of an AC circuit can be calculated by a fraction of  $V_{RMS}$  and  $I_{RMS}$  (Eq. (1)).

$$\text{Impedance of AC circuit (Z), } Z(\Omega) = \frac{V_{RMS}(V)}{I_{RMS}(A)} \quad (1)$$

The composition of gas products was analyzed by a gas chromatograph (GC, Younglin YL6100GC) with a Carboxen™ 1010 PLOT capillary column as the GC column. The GC system was used with a thermal conductivity detector (TCD) and flame ionization detector (FID) as detectors. The GC analysis detected the gas product of the reaction, which included CO, CO<sub>2</sub>, and CHF<sub>3</sub>. Diagnos-

<sup>†</sup>To whom correspondence should be addressed.

E-mail: wglee@kangwon.ac.kr

Copyright by The Korean Institute of Chemical Engineers.

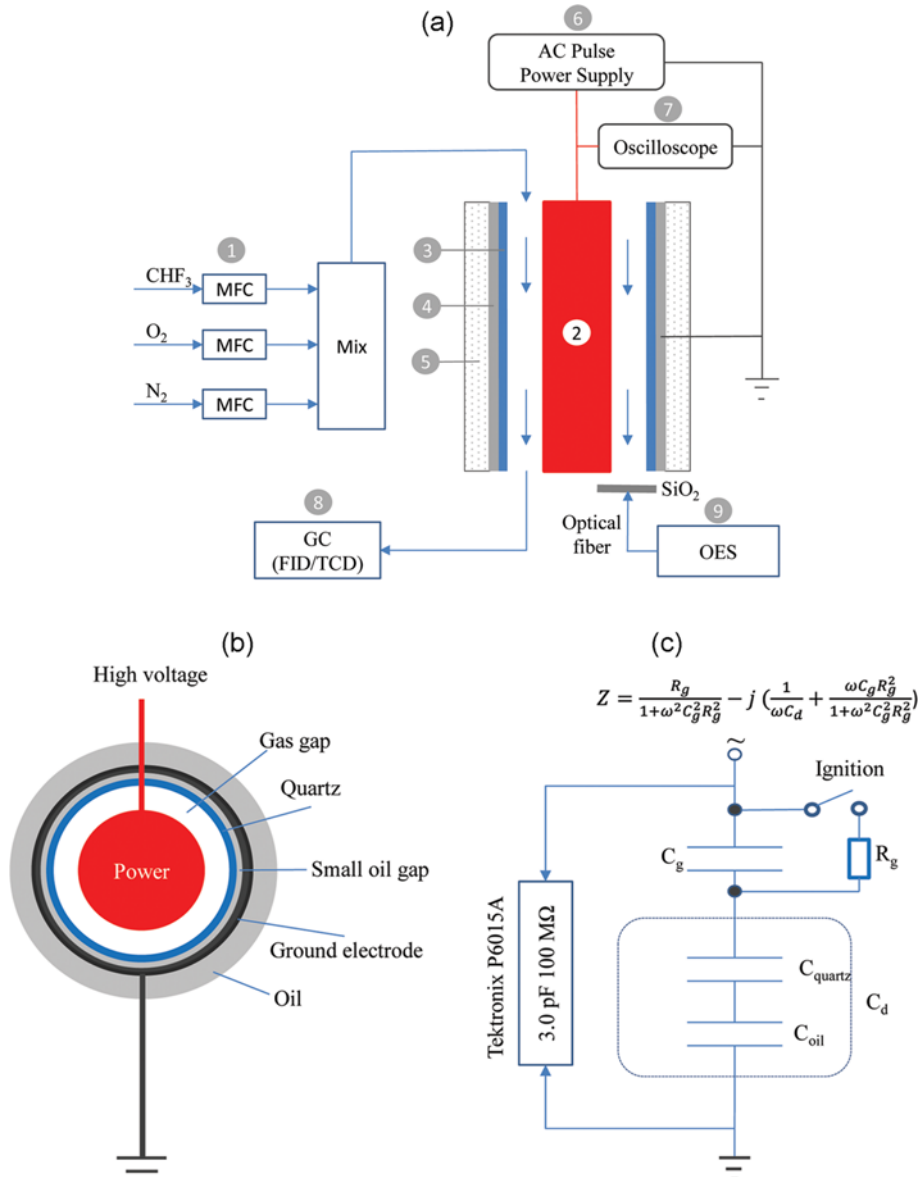


**Fig. 1.** (a) Schematic diagram of experimental setup, with 1=mass flow controller, 2=power electrode, 3=quartz tube, 4=ground electrode, 5=electrically insulating oil, 6=AP plasma power supply, 7=Tektronix 2012B used P6015A passive high voltage probe, 8=gas chromatograph (Younglin YL6100GC), 9=optical emission spectroscopy (AvaSpec-2048 XL), (b) cross-sectional view of reactor, and (c) equivalent circuit model, with R<sub>g</sub>=equivalent resistance of the reactor, C<sub>g</sub>=capacitance of the discharge gap, C<sub>quartz</sub>=capacitance of quartz, C<sub>oil</sub>=capacitance of oil, C<sub>d</sub>=absolute capacitance of the dielectric layers. Small oil gap induced by incomplete contact between ground electrode and outer surface of quartz tube has an equivalent circuit as follows:  $(1/C_d) = (1/C_{quartz}) + (1/C_{oil})$ .

sis of the (CHF<sub>3</sub>, O<sub>2</sub>, N<sub>2</sub>) plasma reaction was measured by an optical emission spectroscopy (AvaSpec-2048 XL). The overall decomposition, selectivity, energy efficiency, and energy density were defined as follows:

$$\text{Decomposition of CHF}_3 (\%) = \frac{C_{CHF_3}(\text{in}) - C_{CHF_3}(\text{out})}{C_{CHF_3}(\text{in})} 100\% \quad (2)$$

$$\text{Selectivity of CO (\%)} = \frac{C_{CO}(\text{out})}{C_{CHF_3}(\text{in}) - C_{CHF_3}(\text{out})} 100\% \quad (3)$$

$$\text{Selectivity of CO}_2 (\%) = \frac{C_{CO_2}(\text{out})}{C_{CHF_3}(\text{in}) - C_{CHF_3}(\text{out})} 100\% \quad (4)$$

Selectivity of by-products (%)

$$= \frac{C_{CHF_3}(\text{in}) - C_{CHF_3+CO+CO_2}(\text{out})}{C_{CHF_3}(\text{in}) - C_{CHF_3}(\text{out})} 100\% \quad (5)$$

$$\text{Energy Efficiency, EE} \left( \frac{\text{mmol}}{\text{kJ}} \right) = \frac{F[C_{CHF_3}(\text{in}) - C_{CHF_3}(\text{out})] \left( \frac{\text{ml}}{\text{min}} \right)}{24.04 \left( \frac{\text{ml}}{\text{mmol}} \right) P \left( \frac{\text{kJ}}{\text{min}} \right)} \quad (6)$$

$$\text{Energy Density, ED} \left( \frac{\text{kWh}}{\text{Nm}^3} \right) = \frac{P(\text{kW})}{F \left( \frac{\text{Nm}^3}{\text{h}} \right)} \quad (7)$$

The gas volume of 1 mmol was 24.04 ml at a standard temperature

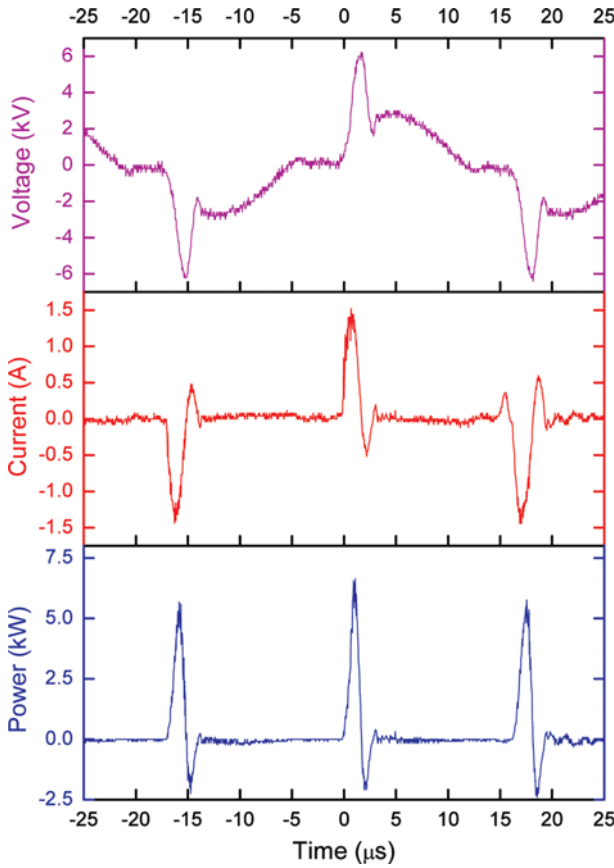


**Fig. 2.** Typical waveforms of voltage, current and discharge power (flow rate of CHF<sub>3</sub>, O<sub>2</sub> and total was 5, 10 and 1,000 ml/min, respectively; frequency=30 kHz; applied voltage=6.7 kVp).

and pressure.

## RESULTS AND DISCUSSION

### 1. Optical Emission Spectrum of Plasma Discharge

The emission spectrum of a mixture of CHF<sub>3</sub>, N<sub>2</sub>, and O<sub>2</sub> plasma reaction in a DBD was measured. The reactor had a quartz tube connected to a male threaded pipe for outside the oil bath. The tip of the optical cable was protected by the covering with a quartz plate, which prevented etching by fluorine species. The plasma reaction was performed under the following conditions: applied voltage of 6.7 kVp, frequency of 30 kHz; total gas flow rate of 1,000 ml/min (CHF<sub>3</sub>:O<sub>2</sub>:N<sub>2</sub>=5:10:985). The identification of the emission spectrum in the wavelength from 200 to 750 nm is shown in Fig. 3. It demonstrates that the emission of N<sub>2</sub> (C <sup>3</sup>Π<sub>u</sub>→B <sup>2</sup>Π<sub>g</sub>) had high intensity, whereas other species had weak intensity: N<sub>2</sub> (B <sup>3</sup>Π<sub>g</sub>→A <sup>3</sup>Σ<sub>u</sub><sup>+</sup>), CF, CF<sub>2</sub>, NO, C<sub>2</sub>, CO, F, and H<sub>2</sub> band. Unfortunately, typical emission peaks of CF<sub>4</sub>, CF<sub>3</sub>, CH, CO<sub>2</sub>, O, H<sub>α</sub>, OH, H<sub>2</sub>O, and O<sub>2</sub> species could not be clearly detected. Spectrum analysis could explain the reaction pathway of the decomposition of CHF<sub>3</sub> in the mixture of CHF<sub>3</sub>, O<sub>2</sub>, and N<sub>2</sub> at DBD conditions as shown in Fig. 4, which is consistent with a previous report [15]. It demonstrated that the decomposition of CHF<sub>3</sub> and selectivity of products depended on the number of active electrons, oxygen species, and O<sub>2</sub> concentration level. The main by-products of the plasma reaction among CHF<sub>3</sub>, O<sub>2</sub> and N<sub>2</sub> were CO and CO<sub>2</sub>. However, the gases CF<sub>4</sub>, C<sub>2</sub>F<sub>2</sub>, C<sub>4</sub>F<sub>4</sub>, C<sub>2</sub>F<sub>6</sub>, COF<sub>2</sub>, F<sub>2</sub>, H<sub>2</sub>, NO, and H<sub>2</sub>O were also detected as the by-products of the plasma reaction, even though the amounts were very small.

### 2. Effect of Input Parameters on Reaction

A plasma reaction depends on the input parameters such as the

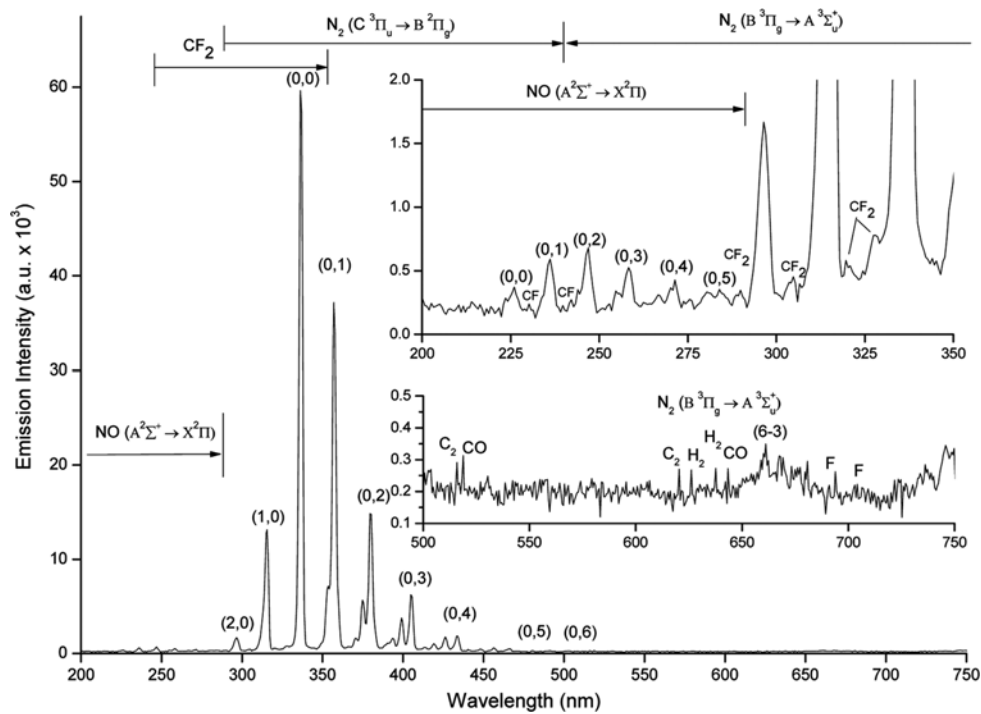


**Fig. 3.** Emission spectrum of (CHF<sub>3</sub>, N<sub>2</sub>, O<sub>2</sub>) plasma in the range of 200-750 nm (total flow rate=1,000 ml/min; flow rate of CHF<sub>3</sub> in feed=5 ml/min; flow rate of O<sub>2</sub> in feed=10 ml/min; frequency=30 kHz; applied voltage=6.7 kVp).

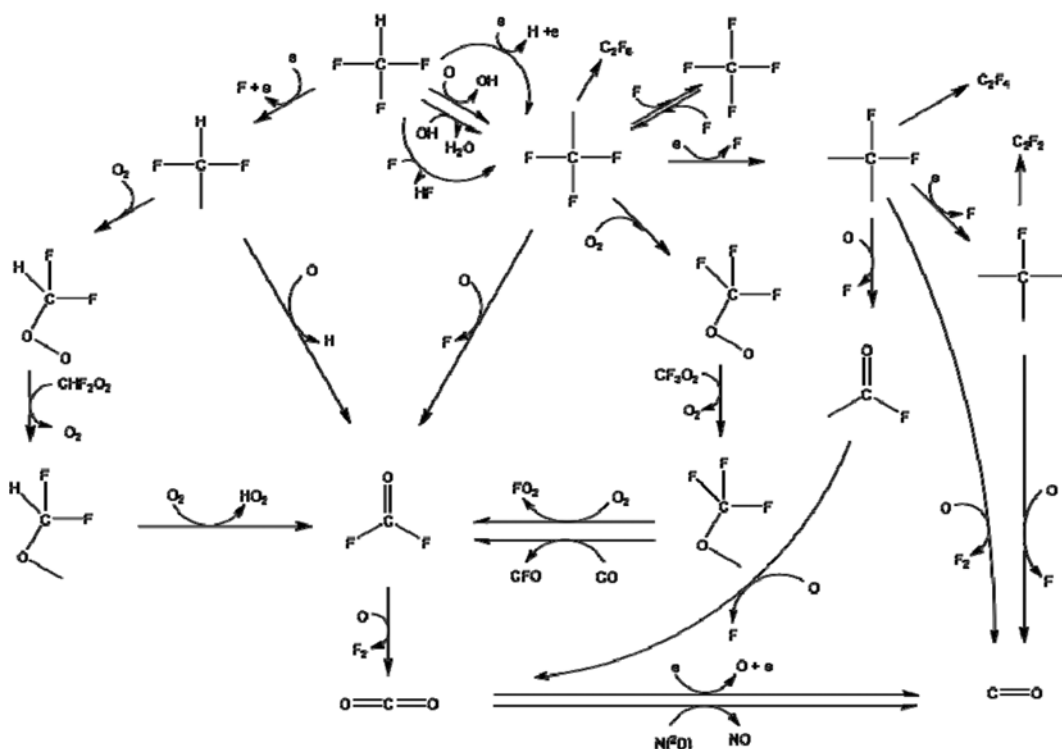


Fig. 4. Possible reaction pathways for conversion of CHF<sub>3</sub> in (CHF<sub>3</sub>, O<sub>2</sub>, N<sub>2</sub>) plasma.

applied voltage, CHF<sub>3</sub> flow rate, and total flow rate. In this study, the decomposition of CHF<sub>3</sub> in the DBD was investigated at various parameters: applied voltage (5.7–7.3 kVp), flow rate of CHF<sub>3</sub> (3–9 ml/min), and total flow rate (500–2,000 ml/min).

The strength of the internal electrical field in plasma reactions is related to the magnitude of the applied voltage. The effect of applied voltage on the plasma reaction was examined with the various applied voltages from 5.7 to 7.3 kVp. Fig. 5(a) shows that the discharge power and the reactor temperature increased with an increase in applied voltage from 5.7 to 7.3 kVp. At the applied voltage of 7.3 kVp, the power and the temperature reached 300 W and 138 °C. The

decomposition of CHF<sub>3</sub> occurred sharply with an increase of applied voltage, which had the same trend as the delivered power according to the applied voltage as shown in Fig. 5(b). CHF<sub>3</sub> was completely decomposed at applied voltage  $\geq 7.0$  kVp. The selectivity of CO<sub>2</sub> slightly increased, whereas the selectivity of CO decreased with the applied voltage. However, the selectivity of the by-products did not change significantly in the range of applied voltage.

The effect of the CHF<sub>3</sub> flow rate on the reaction was investigated by varying the CHF<sub>3</sub> flow rate from 3 to 9 ml/min in the feed. The plasma reaction was performed at an applied voltage of 6.7 kVp, a fixed O<sub>2</sub> flow rate of 10 ml/min and a total flow rate of 1,000 ml/

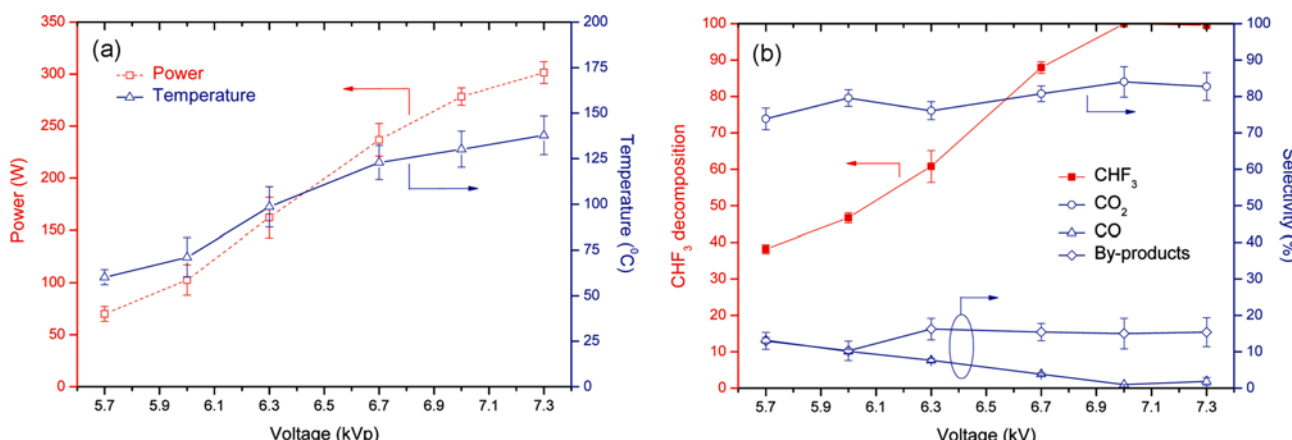


Fig. 5. Effect of applied voltage on the (a) surface temperature of ground electrode surface and discharge power, and (b) CHF<sub>3</sub> decomposition and selectivity of products (flow rate of CHF<sub>3</sub>, O<sub>2</sub> and total in the feed of 5, 10 and 1,000 ml/min, respectively; frequency=30 kHz; reactor temperature was average ten times during plasma reaction of 15 min).

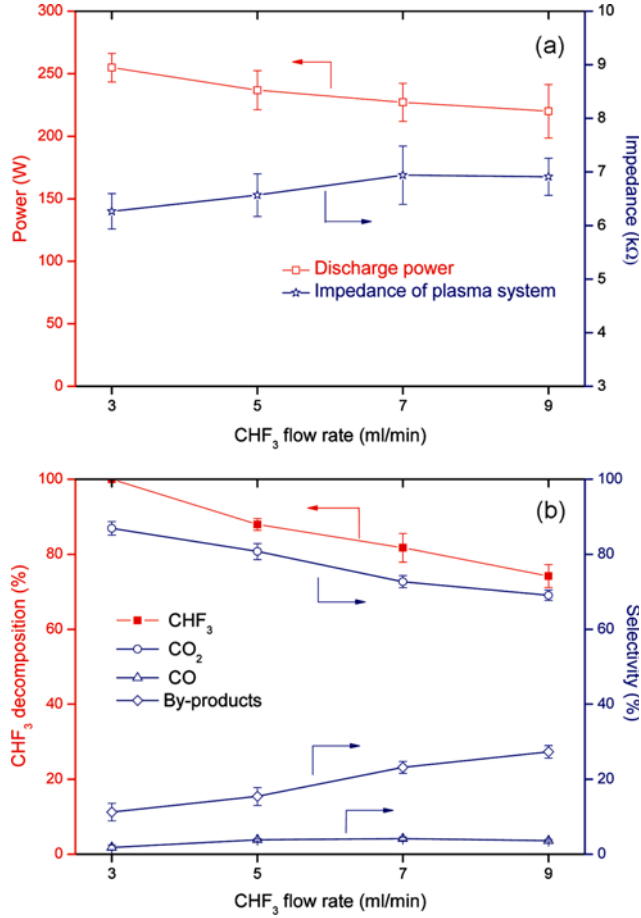


Fig. 6. Effect of  $\text{CHF}_3$  flow rate on (a) discharge power and impedance of plasma system, and (b)  $\text{CHF}_3$  decomposition and selectivity of products (flow rate of  $\text{O}_2$  and total in the feed of 10 and 1,000 ml/min, respectively; power frequency=30 kHz; applied voltage=6.7 kVp).

min. Fig. 6 shows that the discharge power, decomposition of  $\text{CHF}_3$ , and selectivity of  $\text{CO}_2$  decreased linearly with an increase in the  $\text{CHF}_3$  flow rate from 3 to 9 ml/min, while the selectivity of by-products increased with an increase in the  $\text{CHF}_3$  concentration in the feed. The discharge power decreased from 254.8 to 219.9 W when the  $\text{CHF}_3$  flow rate was varied from 3 to 9 ml/min. This result might be related to the amount of equivalent resistance of the reactor ( $R_g$ ). The discharge power can be given by Eq. (8) [16,17]:

$$P = V_{\text{RMS}}^2 \frac{1}{R_g \left(1 + \frac{C_g}{C_d}\right)^2 + \frac{1}{\omega^2 C_d^2 R_g}} \quad (8)$$

where,

$V_{\text{RMS}}$  is the root mean square of the voltage

$R_g$  is the equivalent resistance of the reactor

$C_g$  is the capacitance of the discharge gap

$C_d$  is the absolute capacitance of the dielectric layers

The impedance of the plasma circuit,  $Z = (R_g/1 + \omega^2 C_g^2 R_g^2) - j((1/\omega C_d) + (\omega C_g R_g^2/1 + \omega^2 C_g^2 R_g^2))$  increased slightly from 6264.95 to 6910.90  $\Omega$  with the initial flow rate of  $\text{CHF}_3$  as shown in Fig. 6(a).

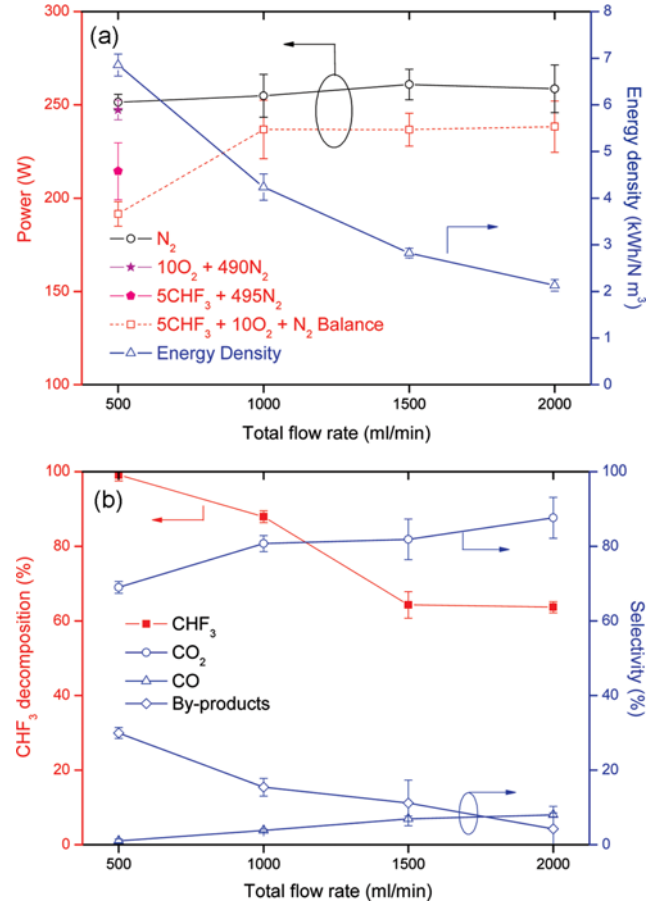


Fig. 7. Effect of total flow rate on (a) discharge power and energy density, and (b)  $\text{CHF}_3$  decomposition and selectivity of products (flow rate of  $\text{CHF}_3$  and  $\text{O}_2$  in feed of 5 and 10, respectively; power frequency=30 kHz; applied voltage=6.7 kVp).

An increase of  $\text{CHF}_3$  concentration in the feed decreased the decomposition of  $\text{CHF}_3$  from 100% to 74.2% as shown in Fig. 6(b). The selectivity of  $\text{CO}_2$  decreased with an increase in the  $\text{CHF}_3/\text{O}_2$  ratio in the feed from 3/10 to 9/10. Gandhi et al. [15] suggested that the concentration of CO and  $\text{CO}_2$  in the by-products increased with an increase in the  $\text{O}_2$  concentration in the feed. The decomposition of  $\text{CHF}_3$  was completed at a  $\text{CHF}_3$  flow rate of 3 ml/min and exhibited a selectivity of CO and  $\text{CO}_2$  of 1.84% and 86.91%, respectively.

The discharge power decreased significantly at a total flow rate of 500 ml/min with a mixture of  $5\text{CHF}_3+10\text{O}_2+485\text{N}_2$  as shown in Fig. 7(a). The decrease in discharge power was related to the presence of  $\text{CHF}_3$  rather than  $\text{O}_2$ , which strongly showed the dependency of the discharge power on the gas composition. The decomposition of  $\text{CHF}_3$  and the selectivity of by-products depended on the total flow rate, as shown in Fig. 7(b). The decomposition of  $\text{CHF}_3$  decreased sharply from 99.15% to 63.70% when the total flow rate changed from 500 to 2,000 ml/min. This result would be related to the residence time of gas in the plasma reactor.

### 3. Energy Efficiency

To compare the effect of the parameters, applied voltage,  $\text{CHF}_3$  flow rate and total flow rate, the energy efficiency was calculated

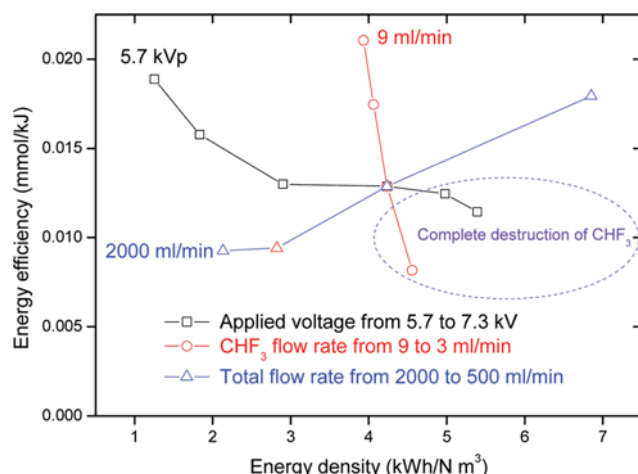


**Fig. 8. Effect of energy density on the energy efficiency with variation of applied voltage; CHF<sub>3</sub> and total flow rate (frequency = 30 kHz).**

as a function of energy density as shown in Fig. 8. For applied voltage, the energy density increased with the applied voltage, whereas the energy efficiency became increased at a lower energy density. The energy efficiency decreased sharply in the narrow width of energy density according to the variation of the CHF<sub>3</sub> flow rate. The energy density related to the total flow rate decreased with the amount of total flow rate, and the energy efficiency increased with a decreasing total flow rate. These results demonstrated that the processes with a relatively higher energy efficiency could be performed at a lower applied voltage, a higher concentration of CHF<sub>3</sub>, and a lower total flow rate. A complete decomposition of CHF<sub>3</sub> occurred at the following process conditions: an applied voltage  $\geq 7.0$  kVp with a CHF<sub>3</sub> flow rate up to 5 ml/min. The energy efficiency was approximately 0.0125 mmol/kJ.

A comparison of energy efficiency with the Gandhi et al's [15] report is shown in Table 1, which contains the degree of CHF<sub>3</sub> decomposition in a DBD with and without packing materials. The reported plasma system has intentionally used a heating tape to sustain some degree of surface temperature, whereas, in our plasma system, a heating system was not adopted. The level of process temperatures is compared in Table 1. For the complete destruction of CHF<sub>3</sub>, the energy efficiency in our work was comparable to, or higher than, the value in Gandhi's report. The difference may have been due to the improved method for delivering power into the discharge zone when a DBD was immersed in an insulating

oil bath [18].

## CONCLUSION

CHF<sub>3</sub> decomposition in a mixture of CHF<sub>3</sub>, O<sub>2</sub>, and N<sub>2</sub> was performed using a DBD immersed in an insulating oil. The effect of applied voltage, CHF<sub>3</sub> flow rate and total flow rate on CHF<sub>3</sub> decomposition was investigated in terms of the discharge power, temperature of the ground electrode surface, energy density, energy efficiency, conversion of CHF<sub>3</sub>, and selectivity of products (CO, CO<sub>2</sub> and byproducts). CHF<sub>3</sub> decomposition increased with a decrease in the CHF<sub>3</sub> flow rate and the total flow rate, and an increase in applied voltage, depending on the amount of discharge power. The selectivity of carbon oxide compounds increased significantly with an increase in the N<sub>2</sub> flow rate. Energy efficiency was higher with a higher CHF<sub>3</sub> concentration or lower total flow rate. The value of energy efficiency and energy density at the center range for the complete CHF<sub>3</sub> decomposition was 0.01 mmol/kJ and 6.00 kWh/Nm<sup>3</sup>, respectively.

## ACKNOWLEDGEMENTS

This work was supported by the National Research Foundation of Korea (NRF) grant funded by the Korean Government (NRF-2013R1A1A2005014).

## REFERENCES

- J. T. Houghton, Y. Ding, D. J. Griggs, M. Noguer, P. J. van der Linden, X. Dai, K. Maskell and C. Johnson, *Climate change 2001: the scientific basis*, Cambridge University Press (2001).
- W. Han, E. M. Kennedy, S. K. Kundu, J. C. Mackie, A. A. Adesina and B. Z. Dlugogorski, *J. Fluorine Chem.*, **131**, 751 (2010).
- P. Zhang, L. Cao, R. Pan, Z. Jiang, K. Qin and Q. Li, *Procedia Eng.*, **62**, 337 (2013).
- A. Vakulka, G. Tavčar and T. Skapin, *J. Fluorine Chem.*, **142**, 52 (2012).
- W. Han, Y. Chen, B. Jin, H. Liu and H. Yu, *Greenhouse Gas Sci. Technol.*, **4**, 121 (2014).
- Y. S. Mok, *Destruction of fluorinated greenhouse gases by using non-thermal plasma process*, INTECH Open Access Publisher (2011).
- S. Choi, K. Y. Cho, J. M. Woo, J. C. Lim and J. K. Lee, *Curr. Appl. Phys.*, **11**, S94 (2011).
- W. Han, E. M. Kennedy, J. C. Mackie and B. Z. Dlugogorski, *J. Haz-*

**Table 1. Comparison of energy efficiency in CHF<sub>3</sub> decomposition by a dielectric barrier discharge reactor**

System	Pack. mater.	CHF <sub>3</sub> /O <sub>2</sub> /Total (ml/min)	T °C	Power W	C %	EE mmol/kJ	Ref.
DBD in air	Al <sub>2</sub> O <sub>3</sub>	1/10/500	298	90	100	0.0083	Gandhi et al. [15]
	ZrO <sub>2</sub>	1/10/500	319	60	100	0.0120	
	No	1/10/500	258	60	71	0.0088	
DBD in oil	No	3/10/1000	70	255	100	0.0082	This work
	No	5/10/1000	80	278	100	0.0125	

EE: energy efficiency (Eq. (6)); T: surface temperature of ground electrode; C: conversion

- ard. Mater.*, **180**, 181 (2010).
9. UNFCCC, “Validation projects methodologies: AM0001”, Unfccc (2015).
10. A. McCulloch, *Background\_240305. pdf [Accessed 15 April 2010]* (2005).
11. D. H. Kim, Y. S. Mok, S. B. Lee and S. M. Shi, *J. Adv. Oxid. Technol.*, **13**, 36 (2010).
12. B. A. Wofford, M. W. Jackson, C. Hartz and J. W. Bevan, *Environ. Sci. Technol.*, **33**, 1892 (1999).
13. D. H. Kim, Y. S. Mok and S. B. Lee, *Thin Solid Films*, **519**, 6960 (2011).
14. D. B. Nguyen and W. G. Lee, *Korean J. Chem. Eng.*, **32**, 62 (2015).
15. M. S. Gandhi and Y. S. Mok, *J. Environ. Sci.*, **24**, 1234 (2012).
16. K. Kostov, R. Y. Honda, L. Alves and M. Kayama, *Braz. J. Phys.*, **39**, 322 (2009).
17. D. B. Nguyen and W. G. Lee, *J. Ind. Eng. Chem.*, **32**, 187 (2015).
18. D. B. Nguyen and W. G. Lee, *J. Ind. Eng. Chem.*, **20**, 972 (2014).